STUDY OF STRUCTURE, HYDROGEN ABSORPTION AND ELECTROCHEMICAL PROPERTIES OF $Ti_{0.5}Zr_{0.5}Ni_yV_{0.5}Mn_x$ SUBSTOICHIOMETRIC LAVES PHASE ALLOYS

T.A. ZOTOV, V.N. VERBETSKY, O.A. PETRII, T.Y. SAFONOVA
Moscow State University, Department of Chemistry,
Leninskie Gory 3, Moscow, 119992 Russia
E-mail: Verbetsky@hydride.chem.msu.ru

Abstract

We continue our previous study [14, 15] of hydrogen absorption and electrochemical properties of $Ti_{0.5}Zr_{0.5}Ni_yV_{0.5}Mn_x$ nonstoichiometric Laves phase alloys. Two series of alloys $Ti_{0.5}Zr_{0.5}Ni_{1.0}V_{0.5}Mn_x$ (x = 0.1- 0.4, $AB_{1.6}$ – $AB_{1.9}$) and $Ti_{0.5}Zr_{0.5}Ni_{1.15}V_{0.5}Mn_x$ (x = 0.1-0.55, $AB_{1.75}$ – $AB_{2.2}$) were prepared and investigated. Their electrochemical discharge characteristics were compared with results of $Ti_{0.45}Zr_{0.55}Ni_{0.7}V_{0.45}Mn_x$ (x = 0.1-1.5, $AB_{1.25}$ – $AB_{2.6}$) and $Ti_{0.45}Zr_{0.55}Ni_{0.85}V_{0.45}Mn_x$ (x = 0.1 1.35, $AB_{1.4}$ – $AB_{2.65}$) alloys corresponding to our previous study. It was shown, that the rate capability increases as the nickel content in alloy series increases. However the discharge capacity of $Ti_{0.5}Zr_{0.5}Ni_{1.0}V_{0.5}Mn_x$ alloys doesn't significantly increase as compared with $Ti_{0.45}Zr_{0.55}Ni_{0.85}V_{0.45}Mn_x$ alloys. Moreover, the discharge capacity decreases with the further increase in the nickel content in $Ti_{0.5}Zr_{0.5}Ni_{1.15}V_{0.5}Mn_x$ alloys. The values of discharge capacities at discharge current densities 100 mA/g are in a range of 310 – 390 mAh/g.

Keywords: MH electrodes, intermetallic compounds (IMC), crystal structure, hydrogen absorption, discharge capacity

1. Introduction

Nickel metal hydride (Ni-MH) batteries are widely adopted today due to their significant discharge capacity, high rate discharge ability (rate capability) and environmental safety [1, 2]. Numerous investigations were concerned with the application of the Laves phase intermetallic compounds (IMC) in Ni-MH technology in the recent time [1-9]. Ti-Zr-Ni-V-Mn Laves phase alloys demonstrate rather good hydrogen absorption and electrochemical properties [1-9]. However, at present, the influence of nickel and manganese on hydrogen absorption and electrochemical characteristics is not quite studied and systematized.

Two maximums of electrochemical discharge capacity for $Ti_{0.45}Zr_{0.55}Ni_{0.7}V_{0.45}Mn_x$ (x = 0.1-1.5, $AB_{1.25}$ – $AB_{2.6}$) and $Ti_{0.45}Zr_{0.55}Ni_{0.85}V_{0.45}Mn_x$ (x = 0.1-1.3; $AB_{1.4}$ – $AB_{2.6}$) systems were found to correspond to the compositions about $AB_{1.5}$ and AB_2 [14, 15]. $Ti_{0.45}Zr_{0.55}Ni_{0.85}V_{0.45}Mn_x$ alloys showed better electrochemical characteristics [14-15].

T.N. Veziroglu et al. (eds.),
Hydrogen Materials Science and Chemistry of Carbon Nanomaterials, 569-577.

Thus, it is of interest to investigate this system in the substoichiometric region ($AB_{<2}$) with higher nickel content. The two series of alloys $Ti_{0.5}Zr_{0.5}Ni_{1.0}V_{0.5}Mn_x$ (x = 0.1- 0.4, $AB_{1.6}$ – $AB_{1.9}$) and $Ti_{0.5}Zr_{0.5}Ni_{1.15}V_{0.5}Mn_x$ (x = 0.1-0.55, $AB_{1.75}$ – $AB_{2.2}$) were prepared for this purpose.

2. Experimental

Alloys were prepared by arc-melting the mixtures of pure initial metals under argon atmosphere. With the purpose of homogenization, the alloys were annealed for 240 h at 850°C in quartz ampoule under vacuum with subsequent quenching in cold water. The phase composition of alloys was examined on polished cross sections of the ingots by a scanning electron microscope (SEM) with an energy dispersive X-ray analyzer (EDXA JXA-733 with LINK-2 microcomputer system). The crystal structure and lattice parameters were determined by means of powder X-ray diffraction (URD-6 diffractometer with CuK). Conditions were: scan range 25-85 (2θ) with a step of 0.02^0 (2θ) and a sampling time of 1 second per step. The refinement of diffraction profiles was performed using the Rietveld method [13].

The hydrogen absorption properties were studied by measuring PCT isotherms using a Siewert's type apparatus at a hydrogen pressure below 50 atm.

The electrochemical discharge properties were studied using an automatic galvanostat connected with a personal computer. The electrochemical experiments were carried out in a three-electrode electrochemical glass cell with Hg/HgO electrode as the reference. The electrolyte was 6 M KOH solution. The MH electrodes were prepared by cold-pressing of the mixture of IMC hydride powder (20%) with copper powder (80%) in a pellet. The preliminary activation of MH electrodes involved boiling in 6 M KOH at about 115°C for 1.5 h before the first polarization. The activation conditions were chosen accordingly [12] study. It was found that after preliminary activation the discharge capacity of MH electrodes studied reaches its maximum in 2—4 cycles. Samples were charged at a current density of 100 mA/g for 4 - 6 h. The discharge cut-off potential was – 650 mV against the Hg/HgO electrode. The discharge capacity was checked at current densities of 100, 200, 400, and 600 mA/g. The rate capability of the samples was estimated as ratio of the discharge capacities at 400 and 100 mA/g current densities.

3. Results and discussion

The results obtained by using electron microscopy, electron probe microanalysis, and powder X-ray diffraction analysis indicate that samples were single phase pseudo binary IMC with Laves phase C14 structure. The small amount (1 – 2%) of nonstoichiometric zirconium oxide with cubic lattice (Fm3m, 225) is present in all alloys. The lattice parameters of the C14 Laves phase were found to decrease with an increase in the manganese content in the alloys series and the coefficient "n" in AB_n (Tab. 1).

The element distribution in the Laves phase structure in $Ti_{0.5}Zr_{0.5}Ni_{1.0\text{-}1.15}V_{0.5}Mn_x$ series is similar to our previous $Ti_{0.45}Zr_{0.55}Ni_{0.7\text{-}0.85}V_{0.45}Mn_x$ series [14, 15]. It is known [4, 10, 11] that a part of titanium atoms that occupy the positions of A-atoms in the AB_2—Laves structure can also occupy the positions of B-atoms in substoichiometric IMC. In superstoichiometric IMC, a part of manganese atoms can pass from B positions

TABLE 1. Structural characteristics of IMC

Alloy composition	n in AB_n.	Rwp,[1]	S[2]	RF[3]	a, E	c, E	V, E[3]
$Ti_{0.5}Zr_{0.5}Ni_{1.0}V_{0.5}Mn_{0.1}$	$AB_{1.6}$	8.46	1.044	4.03	4.977	8.119	174.19
$Ti_{0.5}Zr_{0.5}Ni_{1.0}V_{0.5}Mn_{0.2}$	$AB_{1.7}$	7.55	1.058	3.45	4.965	8.093	172.76
$Ti_{0.5}Zr_{0.5}Ni_{1.0}V_{0.5}Mn_{0.3}$	$AB_{1.8}$	5.51	1.074	1.95	4.953	8.075	171.53
$Ti_{0.5}Zr_{0.5}Ni_{1.0}V_{0.5}Mn_{0.4}$	$AB_{1.9}$	5.25	1.032	1.73	4.934	8.044	169.59
$Ti_{0.5}Zr_{0.5}Ni_{1.15}V_{0.5}Mn_{0.1}$	$AB_{1.75}$	7.01	1.323	2.24	4.954	8.083	172.02
$Ti_{0.5}Zr_{0.5}Ni_{1.15}V_{0.5}Mn_{0.2}$	$AB_{1.85}$	6.41	1.175	2.15	4.949	8.065	171.10
$Ti_{0.5}Zr_{0.5}Ni_{1.15}V_{0.5}Mn_{0.3}$	$AB_{1.95}$	5.41	1.070	1.67	4.937	8.044	169.78
$Ti_{0.5}Zr_{0.5}Ni_{1.15}V_{0.5}Mn_{0.4}$	$AB_{2.05}$	7.30	1.053	3.50	4.932	8.036	169.28
$Ti_{0.5}Zr_{0.5}Ni_{1.15}V_{0.5}Mn_{0.5}$	$AB_{2.15}$	6.62	1.330	2.24	4.925	8.021	168.48
$Ti_{0.5}Zr_{0.5}Ni_{1.15}V_{0.5}Mn_{0.55}$	$AB_{2.2}$	6.23	1.032	3.60	4.919	8.009	167.82

to A positions [4, 10, 11]. The occupation of metallic sites in the C14 structure was refined by using the Rietveld method. The minimization of R-factors showed that the best fit is achieved for the following model (Tab. 2). In the sub-stoichiometric ($AB_{<2}$) region (Ti, Zr)(Ti, Ni, V, $Mn)_2$ with a low manganese content, it was found that vanadium atoms occupy totally the 2(a) and partially 6(h) sites of the C14 structure; titanium, nickel and manganese atoms occupy the 6(h) sites. The increase of manganese content leads to displacement vanadium atoms from 6(h) sites. The further increase of manganese content result in titanium displacement from 6(h) sites. And lastly, part of manganese atoms pass to 4(f) positions (Tab. 2).

TABLE 2. The C14 structure sites occupancy for $Ti_{0.5}Zr_{0.5}Ni_yV_{0.5}Mn_x$ alloys

Alloy Composition	Position in C14 structure		
	(4f)	(2a)	(6h)
Substoichiometric AB_{2-x}	Ti+Zr	V	Ti+Ni+V+Mn
	Ti+Zr	V+Mn	Ti+Ni+Mn
Stoichiometric AB_2	Ti+Zr	V+Mn	Ni+Mn
Superstoichiometric AB_{2+x}	Ti+Zr+Mn	V+Mn	Ni+Mn

There are 7 types of tetrahedral interstities in C14 Laves phase structure where hydrogen atoms can localize.

However, definite set of interstities preferable for hydrogen occupation exists for Laves phase hydrides with any composition. Thus, most available interstities are 24(l), 12(k_1), 6(h_1) and 6(h_2) with [A_2B_2] tetrahedral type [10, 11]. In our case, we can see that the affinity for hydrogen decreases in tetrahedral interstities, because the content of

[1] $R_{WP} = [(\Sigma_{Wi}[y_i(exp)-y_i(calc)]^2)/(\Sigma_{Wi}[y_i(exp)]^2)]^{1/2}$.

[2] $S = [(\Sigma_{wi}[y_i(exp)-y_i(calc)]^2)/(N-P)]^{1/2}$, (N – number of experimental points, P – number of refined parameters.

[3] $R_F = (\Sigma\,|\,[I(exp)]^{1/2}-[I(calc)]^{1/2}\,|\,)/(\Sigma[I(exp)]^{1/2})$.

hydrogen forming elements (Zr, Ti and V) in 4(f), 2(a) and 6(h) C14 structure positions decreases. We can suppose, that hydrogen capacity and hydride stability will decrease with an increase in the manganese content.

The equilibrium hydrogen pressure increases with an increase in the manganese content in each series (Fig. 1, Tab. 3). $Ti_{0.5}Zr_{0.5}Ni_{1.15}V_{0.5}Mn_{0.55}$ alloy failed to absorb hydrogen at pressure below 50 atm. The slightly increasing hydrogen equilibrium pressure with an increase in the nickel content was observed when the $Ti_{0.5}Zr_{0.5}Ni_{1.0}V_{0.5}Mn_x$ and $Ti_{0.5}Zr_{0.5}Ni_{1.15}V_{0.5}Mn_x$ samples with similar AB_n composition were compared. However, the influence of manganese content on hydrogen equilibrium pressure is stronger than that of nickel content. The addition of nickel slightly decreased the hydrogen capacity as compared with previous series [14, 15]. The total hydrogen capacity of samples is in a range of 1.8 — 1.9 mass. % and apparently independent on the alloy composition. However, the hydrogen capacity of samples at hydrogen pressures of 1-5 atm., corresponding to the charged MH-electrode, is about 1.5 – 1.7 mass. %. The hydrogen weight content decreases as the manganese content increases in these conditions. The comparison of $Ti_{0.5}Zr_{0.5}Ni_{1.0}V_{0.5}Mn_x$ and $Ti_{0.5}Zr_{0.5}Ni_{1.15}V_{0.5}Mn_x$ series shows that an increase in the nickel content results in a hydrogen content decrease.

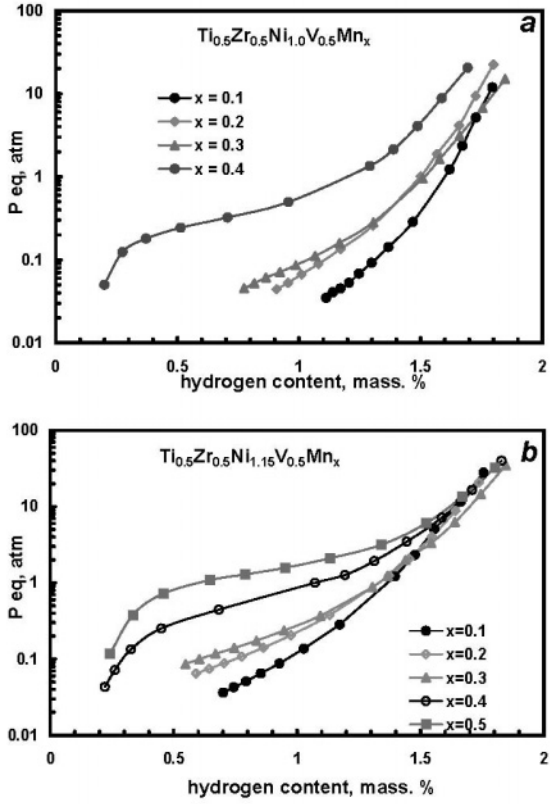

Figure 1. PCT desorption curves for $Ti_{0.5}Zr_{0.5}Ni_{1.0}V_{0.5}Mn_x$ (a) and $Ti_{0.5}Zr_{0.5}Ni_{1.15}V_{0.5}Mn_x$ (b) alloys at room temperature

TABLE 3. Hydrogen absorption and electrochemical properties of $Ti_{0.5}Zr_{0.5}Ni_yV_{0.5}Mn_x$ alloys

Alloy	n in AB_n.	C_{100},[4] mAh/g	Rate capability[5]	H_2 mass. % at 40 atm	P_{eq}[6], atm.	$-\Delta H$, kJ/mol
$Ti_{0.5}Zr_{0.5}Ni_{1.0}V_{0.5}Mn_{0.1}$	$AB_{1.60}$	389	0.86	1.88	<0.01	41.7
$Ti_{0.5}Zr_{0.5}Ni_{1.0}V_{0.5}Mn_{0.2}$	$AB_{1.70}$	323	0.91	1.86	0.04	39.0
$Ti_{0.5}Zr_{0.5}Ni_{1.0}V_{0.5}Mn_{0.3}$	$AB_{1.80}$	339	0.94	1.95	0.09	36.9
$Ti_{0.5}Zr_{0.5}Ni_{1.0}V_{0.5}Mn_{0.4}$	$AB_{1.90}$	355	0.91	1.78	0.32	36.5
$Ti_{0.5}Zr_{0.5}Ni_{1.15}V_{0.5}Mn_{0.1}$	$AB_{1.75}$	350	0.73	1.80	0.05	45.7
$Ti_{0.5}Zr_{0.5}Ni_{1.15}V_{0.5}Mn_{0.2}$	$AB_{1.85}$	335	0.90	1.80	0.14	41.3
$Ti_{0.5}Zr_{0.5}Ni_{1.15}V_{0.5}Mn_{0.3}$	$AB_{1.95}$	318	0.97	1.85	0.15	40.6
$Ti_{0.5}Zr_{0.5}Ni_{1.15}V_{0.5}Mn_{0.4}$	$AB_{2.05}$	327	0.98	1.83	0.64	34.5
$Ti_{0.5}Zr_{0.5}Ni_{1.15}V_{0.5}Mn_{0.5}$	$AB_{2.15}$	307	0.95	1.81	1.58	32.1

From equilibrium pressures at different temperatures (23, 50, 80, 90^0C), the change of enthalpy was estimated according to the Vant-Hoff equation. Table 3 shows that the thermodynamic stability of IMC hydrides decreases with the manganese content and n in AB_n relation increases in each series. The thermodynamic stability of IMC hydrides increases with the nickel content increases.

The discharge curves at current density 100 mA/g are shown in Fig. 2 (except $Ti_{0.5}Zr_{0.5}Ni_{1.15}V_{0.5}Mn_{0.55}$ sample). The change of eqilibrium potential corresponds to an increase in hydride desorption equilibrium pressures in PCT curves. The values of discharge capacities at discharge current densities 100 mA/g are in a range of 310 – 390 mAh/g.

The increase of nickel content involves a decrease in the hydride forming elements (Zr, Ti and V) in alloys. So, the hydrogen capacity of $Ti_{0.5}Zr_{0.5}Ni_{1.0\text{-}1.15}V_{0.5}Mn_x$ alloys is lower than for $Ti_{0.45}Zr_{0.55}Ni_{0.7\text{-}0.85}V_{0.45}Mn_x$ alloys. However, we expected that electrochemical activity would increase with an increase in the nickel content, because in dynamic regime of electrochemical experiment the hydrogen capacity of MH-electrode is only partly realized.

Dependences of discharge capacity on manganese content and B / A ratio are shown in Fig. 3. The shape of the curves for $Ti_{0.5}Zr_{0.5}Ni_{1.0\text{-}1.15}V_{0.5}Mn_x$ samples is similar to that of previous $Ti_{0.45}Zr_{0.55}Ni_{0.7\text{-}0.85}V_{0.45}Mn_x$ series (Fig. 4). In all cases, we have two maximums of discharge capacity at compositions close to $AB_{1.5}$ and AB_2.

[4] Discharge capacity at current density 100mA/g
[5] Rate capability is $C_{i=400}/C_{i=100}$
[6] Desorption equilibrium pressure

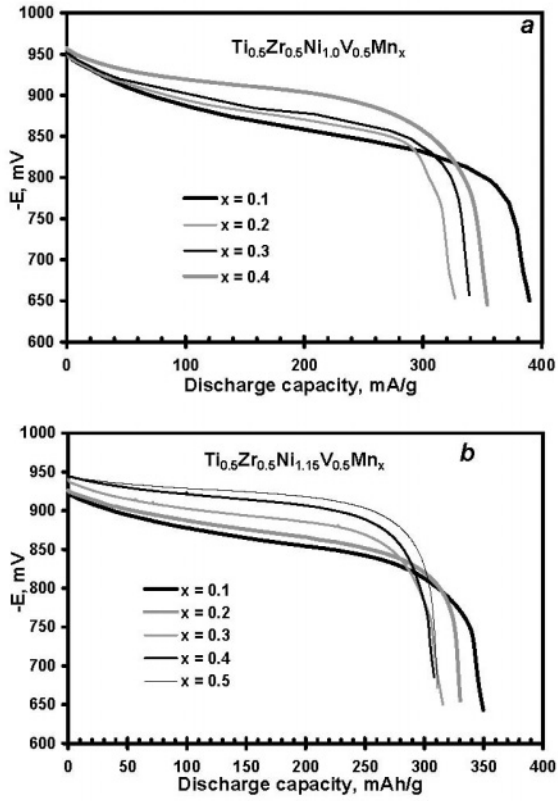

Figure 2. Discharge curves for $Ti_{0.5}Zr_{0.5}Ni_{1.0}V_{0.5}Mn_x$ (a) and $Ti_{0.5}Zr_{0.5}Ni_{1.15}V_{0.5}Mn_x$ (b) alloys at room temperature and current density 100 mA/g

The rate capability of MH-electrodes is characterized by the discharge capacity ratio at current densities of 400 and 100 mA/g. Table 3 shows that the rate capability increases in each series with the manganese content. The rate capability of $Ti_{0.5}Zr_{0.5}Ni_{1.15}V_{0.5}Mn_x$ samples is the highest for the whole $Ti_{0.5}Zr_{0.5}Ni_yV_{0.5}Mn_y$ series. But discharge capacities of $Ti_{0.5}Zr_{0.5}Ni_{1.15}V_{0.5}Mn_x$ samples are lower as compared with $Ti_{0.5}Zr_{0.5}Ni_{1.0}V_{0.5}Mn_x$ samples.

The existing maximums of discharge capacity in alloys series can be explained by the effect of two opposite factors. The first factor decreases the hydrogen capacity with an increase in the manganese content. In contrast, the decrease in thermodynamic stability with an increase in the manganese content leads to an increase in the hydrogen desorption rate and makes electrochemical desorption more complete. This results in the appearance of the maximums, minimums, or "kink" ($Ti_{0.45}Zr_{0.55}Ni_{0.7}V_{0.45}Mn_x$, x = 0.35) of discharge capacities in $Ti_{0.5}Zr_{0.5}Ni_yV_{0.5}Mn_y$ series.

The $Ti_{0.5}Zr_{0.5}Ni_{1.15}V_{0.5}Mn_{0.1}$ sample has a maximum discharge capacity in $Ti_{0.5}Zr_{0.5}Ni_{1.15}V_{0.5}Mn_x$ series at the current density 100 mA/g, but its discharge capacity at 600 mA/g is minimum (C_{400}/C_{100} = 0.73). The decrease of rate capability was observed for $Ti_{0.5}Zr_{0.5}Ni_{1.0}V_{0.5}Mn_{0.1}$ (0.86), $Ti_{0.45}Zr_{0.55}Ni_{0.85}V_{0.45}Mn_{0.25}$ (0.80) and

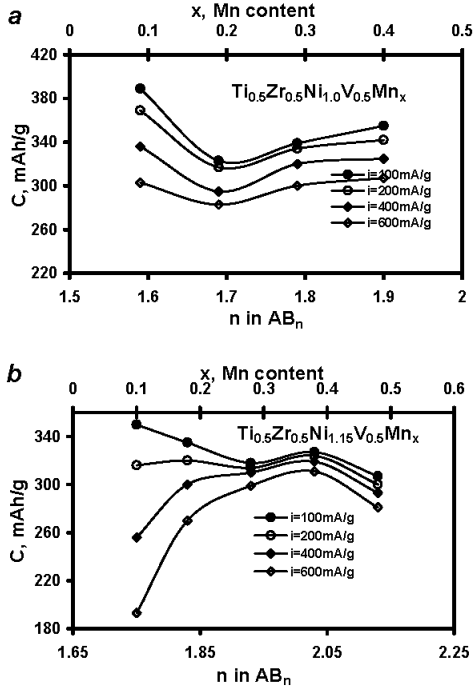

Figure 3. Dependence of discharge capacities of $Ti_{0.5}Zr_{0.5}Ni_{1.0}V_{0.5}Mn_x$ (a) and $Ti_{0.5}Zr_{0.5}Ni_{1.15}V_{0.5}Mn_x$ (b) alloys on manganese content and AB_n relation

$Ti_{0.45}Zr_{0.55}Ni_{0.7}V_{0.45}Mn_{0.35}$ (0.33) alloys, which have maximum ("kink" for $Ti_{0.45}Zr_{0.55}Ni_{0.7}V_{0.45}Mn_{0.35}$) discharge capacity in substoichiometric region of each series (Fig. 3, 4, Tab. 3).

We have $_{shown}$ (Tab. 3), that only two alloys have rather good electrochemical characteristics (C_{100}>350mAh/h; C_{400}/C_{100}>0.85), due to their significant discharge capacity and high rate discharge ability (rate capability). All MH-electrodes were tested in equal experimental conditions (see the experimental part) without studies on the improvement of discharge characteristics. We can suppose, that application of special technique of performance and activating of MH-electrodes can lead to significant improvement of discharge properties for some alloys.

4. Conclusions

The structure, hydrogen absorption and electrochemical properties of $Ti_{0.5}Zr_{0.5}Ni_{1.0\text{-}1.15}V_{0.5}Mn_x$ alloys were studied in this paper which completes the investigation of $Ti_{0.5}Zr_{0.5}Ni_yV_{0.5}Mn_x$ system with Laves phases. Maximums of hydrogen absorption and electrochemical discharge capacities were found for the $Ti_{0.45}Zr_{0.55}Ni_yV_{0.45}Mn_x$ system in stoichiometric composition of about $AB_{1.5}$ and AB_2. The possible explanation to the appearance of the discharge capacity maximum in substoichiometric region was given. The maximum discharge capacity in that region was about 390 mAh/g.

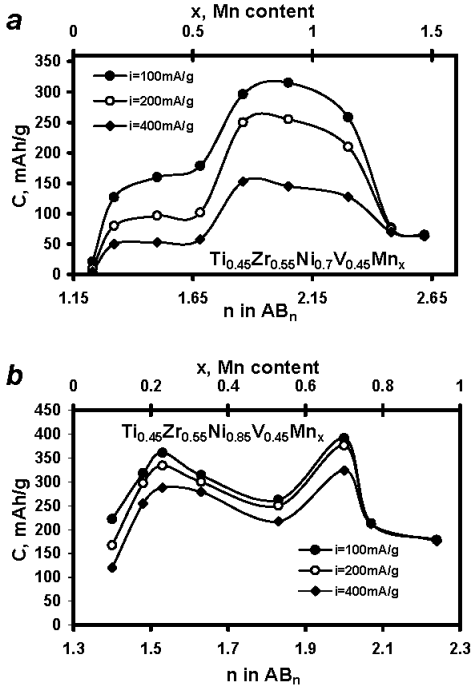

Figure 4. Dependence of discharge capacities of $Ti_{0.45}Zr_{0.55}Ni_{0.7}V_{0.45}Mn_x$ (a) and $Ti_{0.45}Zr_{0.55}Ni_{0.85}V_{0.45}Mn_x$ (b) alloys on manganese content and AB_n relation

5. References

1. Kleperis, J., Wyjcik, G., Czerwinski, A., Skowronski, J., Kopczyk, M. and Beltowska-Brzezinska, M. (2001) Electrochemical behavior of metal hydrides, *J. Solid State Electrochem.* **5**, 229-249.
2. Petrii, O.A., Vasina, S.Ya. and Korobov, I.I. (1996) The electrochemistry of the hydride forming IMC and alloys, *Usp. Khim.* **65**(3), 195-210.
3. Kim, D.-M., Jang, K.-J. and Lee, J.-Y. (1999) A review on the development of AB_2-type Zr-based Laves phase hydrogen storage alloys for Ni-MH rechargeable batteries in the Korea Advanced Institute of Science and Technology, *J. All. Comp.* **293-295**, 583-592.
4. Yoshida, M. and Akiba, E. (1995) Hydrogen absorbing-desorbing properties and crystal structure of the Zr-Ti-Ni-Mn-V AB_2 Laves phase alloys, *J. All. Comp.* **224**, 121-126.
5. Lee, H.-H., Lee K.-Y. and Lee, J.-Y. (1997) The hydrogenation characteristics of Ti-Zr-V-Mn-Ni C14 type Laves phase alloys for metal hydride electrodes, *J. All. Comp.* **253-254**, 601-604.
6. Jung, J.-H., Lee, H.-H., Kim, D.-M., Jang, K.-J. and Lee, J.-Y. (1998) Degradation behavior of Cu-coated Ti-Zr-V-Mn-Ni metal hydride electrodes, *J. All. Comp.* **266**, 266-270.

7. Kim, J.-S., Paik, C.H., Cho, W.I., Cho, B.W., Yun, K.S. and Kim, S.J. (1998) Corrosion behavior of $Zr_{1-x}Ti_xV_{0.6}Ni_{1.2}M_{0.2}$ (M = Ni, Cr, Mn) AB_2-type metal hydride alloys in alkaline solution, *J. Power Sources* **75**, 1-8.
8. Song, X., Zhang, Z., Zhang, X., Lei, Y. and Wang, Q. (1999) Effect of Ti substitution on the microstructure and properties of Zr-Mn-V-Ni AB_2 type hydride electrode alloys, *J. Mater. Res.* **14**(4), 1279-1285.
9. Kim, D.-M., Lee, H., Cho, K. and Lee, J.-Y. (1999) Effect of Cu powder as an additive material on the inner pressure of a sealed-type Ni-MH rechargeable battery using a Zr-based alloy as an anode, *J. All. Comp.* **282**, 261-267.
10. Westlake, D.G. (1983) Hydrides of intermetallic compounds: a revue of stabilities, stoichiometries and preferred hydrogen sites, *J. Less-Common Met.* **91**, 1-20.
11. Yartys, V.A., Burnasheva, V.V., Semenenko, K.N., Fadeeva, N.V. and Solov'ev, S.P. (1982) Crystal chemistry of $RT_5H(D)_x$, $RT_2H(D)_x$ and $RT_3H(D)_x$ hydrides based on intermetallic compounds of $CaCu_5$, $MgCu_2$, $MgZn_2$ and $PuNi_3$ structure types, *J. Hydrogen Energy* **7**(12), 957-965.
12. Verbetsky, V.N., Petrii, O.A., Vasina, S.Ya. and Bespalov, A.P. (1999) Electrode materials based on hydrogen-sorbing alloys of AB_2 composition (A = Ti, Zr; B = V, Ni, Cr), *J. Hydrogen Energy* **24**, 247-249.
13. Izumi, F.A. (1997) Rietveld-refinement program RIETAN-94 for angle-dispersive X-ray and neutron powder diffraction, National Institute for Research in Inorganic Materials, Japan, 35 P.
14. Zotov, T.A., Verbetsky, V.N. and Petrii, O.A. (2002) The Investigation of Hydrogen Absorption and Electrochemical Properties of Alloys Ti-Zr-Ni-V-Mn with Laves Phases in Nonstoichiometric Region, *Hydrogen Materials Science and Chemistry of Metal Hydrides* **82**, 229-234.
15. Petrii, O.A., Mitrokhin, S.V., Verbetsky, V.N. and Zotov, T.A. (2002) Hydrogen absorption and electrochemical properties Ti-Zr-Ni-V-Mn alloys, *Proc. Int. Symp. on Metal Hydrogen Systems*, p. 130.